19th Australasian Fluid Mechanics Conference
Melbourne, Australia
8-11 December 2014

A Compound Cantilevered Plate Model of the Palate-Uvula System during Snoring

J. Cisonni[1], N. S. J. Elliott[1,2], A. D. Lucey[1] and M. Heil[3]

[1]Fluid Dynamics Research Group, Department of Mechanical Engineering
Curtin University, Perth WA 6845, Australia

[2]El Grupo de Investigación de la Dinámica de Fluidos
Xe' lajuj no'j, Guatemala

[3]School of Mathematics
University of Manchester, Manchester M13 9PL, U.K.

Abstract

Flow-induced vibration of the soft tissues of the upper airway is at the origin of snoring noise. For most habitual snorers, the passive motion of the soft palate and its conic projection, the uvula, located at the back of the roof of the mouth, is the main cause of the sleep-related breathing disorder. The flow-induced oscillations of the uvulopalatal system may be modelled using a compound cantilevered flexible plate in a mean channel flow. A parametric study characterises the influence of the mechanical properties of the soft palate and uvula, as well as their relative length, on the flutter-type aeroelastic instability of the plate motion. Results confirm that longer uvulae with typical anatomical properties tend to increase the instability of the FSI system. Further, they show that only much heavier and stiffer uvulae can stabilise the uvulopalatal system and suggest that the tissue properties have to be altered considerably on a large portion of the soft palate to prevent snoring.

Introduction

Snoring is often considered a minor affliction but when heavy is often associated with obstructive sleep apnoea (OSA). This latter condition causes severe sleep deprivation and consequent excessive daytime sleepiness, which is significantly linked to an elevated risk of accidents and cardiovascular disease. The repetitive episodes of hypoventilation and breathing interruptions characterizing OSA are due to flow-induced soft-tissue collapse, partially or completely blocking the upper airway despite an increased breathing effort. Similarly, snoring noise is generated by flow-induced soft-tissue vibration in the upper airway, involving mainly the soft palate and uvula at the back of the roof of the mouth.

Most studies aimed at the prediction of surgical treatment outcomes investigate the effect of compliance of the human soft palate during inspiratory breathing based on anatomically-detailed upper airways reconstructed from medical images [9, 13, 14]. However, these studies have generally used only a very limited number of patient-specific data and uniform elastic properties to model the soft tissue [4]. Therefore, the developed models were only able to provide limited understanding of the physical phenomena and the critical morphological and physiological parameters underlying the pathogenesis.

By contrast, simplified models of the flow-induced motion of the soft palate and the uvula — using a cantilevered flexible plate in a mean channel flow (see figure 1(a)) — elucidate the flutter instability that defines the physical mechanism of snoring [8]. To investigate how the size and material properties of the soft palate and uvula affect their motion and their combined susceptibility to flow-induced oscillation, a modification is made to previously developed models [1, 6, 12]. In a one-dimensional cantilevered flexible plate we vary the flexural rigidity and mass through a plate thickness function (see figure 1(b)). We analyse the fluid-structure interactions (FSI) of this compound plate that comprises two distinct sections, representing the soft palate and the uvula. The cantilever is attached to a rigid wall (hard palate) separating upper (nasal) and lower (oral) inlets of a rigid-walled channel (pharynx) conveying a viscous flow.

The dimensions of the soft palate and uvula can vary considerably between individuals, whether non-snorers, habitual snorers or OSA sufferers [11]. Furthermore, analyses of the velopharyngeal soft tissues have revealed non-uniformities in the elastic properties of the soft palate and uvula [2, 3]. Therefore, a parametric study is conducted to determine the effect of the mechanical properties of the soft palate and uvula, as well as their relative length, on the overall FSI system dynamics.

Methods

The FSI system is composed of a cantilevered flexible plate immersed in a viscous channel flow, as depicted in figure 1(a). The flow with mean inlet velocity U^* in a two-dimensional channel of height H^* and length L^* is governed by the non-dimensional Navier–Stokes equations

$$\mathrm{Re}\left(\frac{\partial u_i}{\partial t}+u_j\frac{\partial u_i}{\partial x_j}\right)=-\frac{\partial p}{\partial x_i}+\frac{\partial}{\partial x_j}\left(\frac{\partial u_i}{\partial x_j}+\frac{\partial u_j}{\partial x_i}\right) \qquad (1)$$

and non-dimensional continuity equation

$$\frac{\partial u_i}{\partial x_i}=0\,, \qquad (2)$$

where $\mathrm{Re}=\rho_f^*\,U^*\,H^*/\mu^*$ is the Reynolds number. All lengths and spatial coordinates are non-dimensionalised on the characteristic length H^*, while time is non-dimensionalised on the natural timescale of the fluid $\mathcal{T}_f^*=H^*/U^*$.

Using the principle of virtual displacements, the deformation of the flexible plate of length l_{flexible} and thickness h is governed by the geometrically non-linear one-dimensional Kirchoff–Love beam equation

$$\int_0^{l_{\mathrm{flexible}}}\left(\gamma\delta\gamma+\frac{h^2}{12}\kappa\delta\kappa-\left(\frac{1}{h}\sqrt{\frac{A}{a}}T_i-\Lambda^2\frac{\partial^2 R_i}{\partial t^2}\right)\delta R_i\right)ds=0\,, \qquad (3)$$

where γ is the axial-strain and κ the bending. The ratio $\sqrt{A/a}$ represents the stretch of the beam's centreline and $ds=\sqrt{a}\,d\xi$ with ξ being the Lagrangian beam coordinate. The non-dimensional parameter

$$\Lambda=\frac{H^*}{\mathcal{T}_f^*}\sqrt{\frac{\rho_s^*}{E_{\mathrm{eff}}^*}}=U^*\sqrt{\frac{\rho_s^*}{E_{\mathrm{eff}}^*}} \qquad (4)$$

Parameter	Symbol	Value
Length of channel	L^*	$120\,mm$
Height of channel	H^*	$20\,mm$
Length of rigid plate	l^*_{rigid}	$20\,mm$
Length of flexible plate	l^*_{flexible}	$40\,mm$
Thickness of flexible plate	h^*	$1\,mm$
Initial plate tip displacement	η^*_0	$25\,\mu m$
Density of plate	ρ^*_s	$1000\,kg{\cdot}m^{-3}$
Elastic modulus of plate	E^*	$25\,kPa$
Poisson's ratio of plate	ν	0.42
Density of fluid	ρ^*_f	$1.1774\,kg{\cdot}m^{-3}$
Dynamic viscosity of fluid	μ^*_f	$1.98\times10^{-5}\,kg{\cdot}m^{-1}{\cdot}s^{-1}$
Mean inlet velocity	U^*	$0.5\,m{\cdot}s^{-1}$
Time step	Dt^*	$1.5\times10^{-3}\,s$
Reynolds number	Re	595
FSI parameter	Q	1.63×10^{-8}
Timescale ratio	Λ^2	8.24×10^{-3}

Table 1: Dimensional and non-dimensional parameters.

is the ratio between the natural timescales of the beam and the fluid, with ρ^*_s being the beam density and $E^*_{\text{eff}} = E^*/(1-\nu^2)$ the effective one-dimensional elastic modulus.

The traction T_i exerted by the flow on the top and bottom surfaces of the flexible plate includes the pressure and viscous loads of the fluid, so that

$$T_i = Q\left(\left(p|_{\text{top}}\hat{N}_i^{[\text{top}]} - \left(\frac{\partial u_i}{\partial x_j} + \frac{\partial u_j}{\partial x_i}\right)\Bigg|_{\text{top}} \hat{N}_j^{[\text{top}]} + \left(p|_{\text{bottom}}\hat{N}_i^{[\text{bottom}]} - \left(\frac{\partial u_i}{\partial x_j} + \frac{\partial u_j}{\partial x_i}\right)\Bigg|_{\text{bottom}} \hat{N}_j^{[\text{bottom}]}\right)\right), \quad (5)$$

where $\hat{N}_i^{[\text{top}]}$ and $\hat{N}_i^{[\text{bottom}]}$ are the outer unit normals on the top and bottom faces of the deformed beam. The ratio

$$Q = \frac{\mu^* U^*}{E^*_{\text{eff}} H^*} \quad (6)$$

between the fluid pressure scale and the beam's effective elastic modulus represents the strength of the fluid-structure interaction and is related to Λ via $\Lambda^2 = (\rho^*_s/\rho^*_f)\,\text{Re}\,Q$.

The problem is formulated using the open-source finite-element library `oomph-lib` [7]. The flexible plate is spatially discretised using two-node Hermite beam elements and the fluid domain using nine-node quadrilateral Taylor-Hood elements with adaptive mesh refinement capabilities. Time stepping is done with a Newmark scheme for the solid and a BDF2 scheme for the fluid. The FSI problem is discretised monolithically and the Newton-Raphson method is used to solve the non-linear system of equations, employing the SuperLU direct linear solver within the Newton iteration. The initialisation procedure involves:

1. prescribing the deformation of the plate into the first *in vacuo* eigenmode with small (linear mechanics) amplitude under no-flow conditions;
2. gradually introducing the flow in a series of steady solutions while constraining the plate in position;
3. unconstraining the plate and solving the unsteady FSI problem.

By investigating different start-up procedures, mesh densities and time step sizes we confirm that the unsteady solutions of the FSI system presented herein are independent of the initial perturbation and spatiotemporal discretisation.

The values corresponding to the parameters shown in figure 1(a) for the reference FSI system (*i.e.* including a uniform-thickness flexible plate) are summarised in table 1. These values are representative of typical anatomical properties of the human velopharynx during snoring [3, 4, 11, 13], creating conditions leading to an unstable reference FSI system.

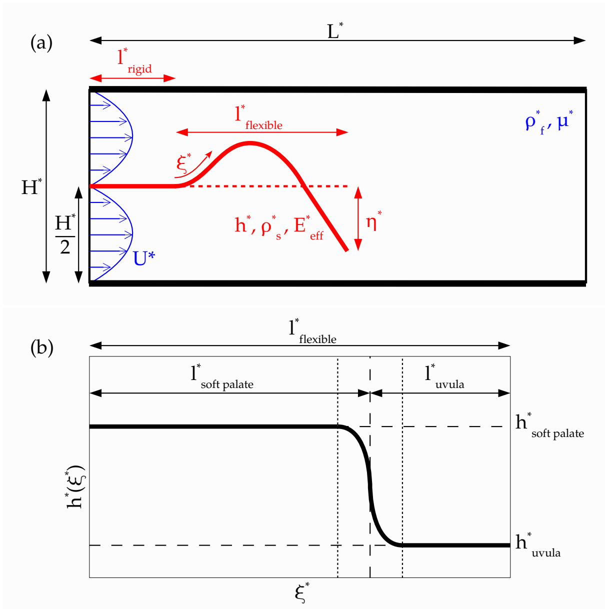

Figure 1: (a) Description of the FSI system modelling: a cantilevered flexible plate immersed in a viscous channel flow, and the physical quantities of the problem. (b) Description of the flexible plate thickness profile showing the two distinct parts corresponding to the soft palate and the uvula.

Results and Discussion

When the reference flexible plate of uniform thickness is immersed in the viscous channel flow, its motion becomes unstable. As shown in figure 2, the tip (free end) of the plate gets further from its equilibrium position with time, and eventually hits the channel wall. The oscillatory motion of the plate follows a regular pattern so that the time trace of the span-wise tip deflection has a unique frequency component, close to the second natural frequency of the plate. Indeed, although the plate is initially deflected in its first mode shape, its second mode is favoured when the flow is introduced in the FSI system, leading to flutter instability. Figure 3(b) illustrates the shape of the deflected plate in the flow at successive time steps over a duration

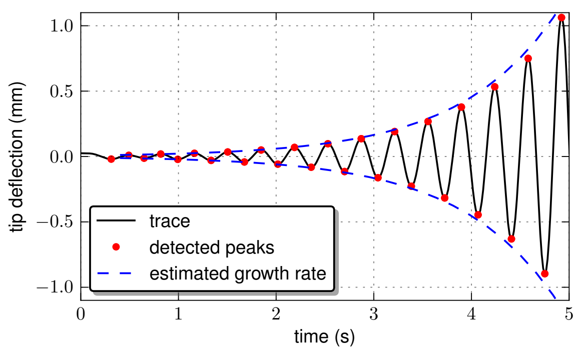

Figure 2: Time trace of span-wise tip deflection for the reference cantilevered flexible plate of uniform thickness $h^* = 1\,mm$ in viscous channel flow. The envelope interpolated with the exponential growth rate estimated from the detected oscillation peaks is also shown.

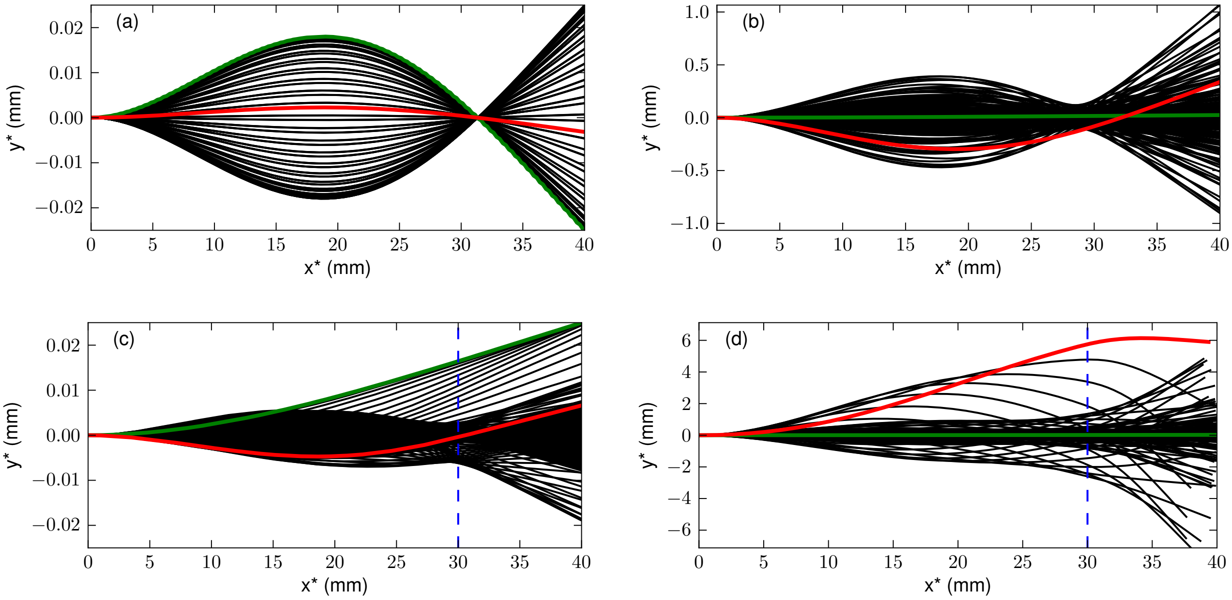

Figure 3: Flexible plate mode shapes for the uniform-thickness plate (a) *in vacuo* and (b) in viscous channel flow, and for non-uniform-thickness plates having $l_{\text{uvula}}/l_{\text{flexible}} = 1/4$ with (c) $h_{\text{uvula}}/h_{\text{soft palate}} = 2$ and (d) $h_{\text{uvula}}/h_{\text{soft palate}} = 1/2$. The bold green and red curves correspond to the first ($t^* = 0\,s$) and last ($t^* = 5\,s$) time steps in each of the sequences plotted. The vertical dashed line in (c) and (d) delineates the limit between soft palate and uvula.

of $5\,s$. It can be seen that the plate mode shape is very similar to the second *in vacuo* mode shape of the same plate, presented in figure 3(a).

The oscillatory motion of compound plates with non-uniform thickness, as qualitatively depicted in figure 1(b), present different patterns which can become very irregular. Figure 3(c,d) show the mode shapes of two plates of which the free end (uvula) has, respectively, an increased thickness $h_{\text{uvula}}/h_{\text{soft palate}} = 2$ and a reduced thickness $h_{\text{uvula}}/h_{\text{soft palate}} = 1/2$ over a length $l_{\text{uvula}}/l_{\text{flexible}} = 1/4$, with the two sections being delineated by a vertical dashed line in each plot. For the thicker uvula model, the second mode shape appears to be also favoured when the flow is introduced in the FSI system but the heavier and relatively more rigid free end has a stabilising effect on the plate. On the other hand, the lighter and more flexible free end of the plate with a thinner uvula destabilises the system. In this case, the second mode is predominant in the motion of the compound flexible plate but higher modes appear to be also significantly excited, particularly when the length $l_{\text{uvula}}/l_{\text{flexible}}$ of the thinner uvula is increased.

The influence of the thickness and length ratios of the uvula relative to the soft palate on the stability of the FSI system is illustrated in figure 4. In this parametric study, the stability of the system for each combination $\{l_{\text{uvula}}/l_{\text{flexible}}\,,\, h_{\text{uvula}}/h_{\text{soft palate}}\}$ is expressed in terms of exponential growth rate determined from the linear fit of the logarithmic variation in amplitude of the time trace of span-wise tip deflection by oscillation period (see figure 2). For all cases, the thickness of the cantilevered end (soft palate) of the plate is kept constant and it can be seen from figure 4 that when the thickness ratio $h_{\text{uvula}}/h_{\text{soft palate}} = 1$, the growth rate remains constant for all the length ratios. With a thinner uvula, the system becomes more unstable as $l_{\text{uvula}}/l_{\text{flexible}}$ increases. In particular, for $h_{\text{uvula}}/h_{\text{soft palate}} \leq 1/2$, the amplification of the plate deflection becomes very rapid for $l_{\text{uvula}}/l_{\text{flexible}} > 0.4$ and the plate hits the channel wall after only two or three oscillations (the determination of a relevant growth rate for these cases is therefore problematic and omitted in the figure). With a thicker uvula, the system becomes less unstable as $l_{\text{uvula}}/l_{\text{flexible}}$ increases. For $1 < h_{\text{uvula}}/h_{\text{soft palate}} \leq 3/2$, the system remains unstable but with a slower plate deflection amplification. However for $h_{\text{uvula}}/h_{\text{soft palate}} \geq 3/2$, the system can be stabilised (negative growth rate) with a sufficiently long uvula. For $h_{\text{uvula}}/h_{softpalate} = 4$, the significantly heavier and more rigid uvula stabilises rapidly the plate motion and the applied initial deflection is damped out within only two or three oscillations.

The range of values of $h_{\text{uvula}}/h_{softpalate}$ and $l_{\text{uvula}}/l_{\text{flexible}}$ used in this parametric study is wider than the typical range of anatomically relevant values for human soft palate and uvula properties. Indeed, typical length ratios of the uvula relative to the soft palate lie below 1/3 and the decrease of effective elastic modulus or rigidity of the uvula compared to the soft palate remains limited [3]. Nonetheless, the results obtained show that in the context of snoring, a thinner, hence lighter and less rigid, uvula increasingly destabilises the soft palate as it gets longer. This agrees with clinical observations showing that habitual snorers have a significantly longer uvula [10]. Moreover, the results obtained for $h_{\text{uvula}}/h_{softpalate} > 1$ show that the rigidity and/or the mass of the uvula have to be substantially increased to start stabilising the soft palate. Another interpretation is that the tissue properties have to be altered considerably on a large portion of the soft palate to prevent snoring. This offers a partial explanation for the low success rate of uvulopalatopharyngoplasty (UPPP) [5] which aims to surgically stiffen the soft-palate tissue.

Conclusions

The FSI system studied that comprises a compound cantilevered plate immersed in a viscous channel flow, based upon typical anatomical properties of human velopharynx provides an insight into the underlying mechanics of snoring. Results show that combinations of uvula length and properties exist that demarcate stabilising and destabilising effects of the uvula on flutter of the uvulopalatal system. A thinner, lighter and less rigid free end at the extremity of the palate, which usually charac-

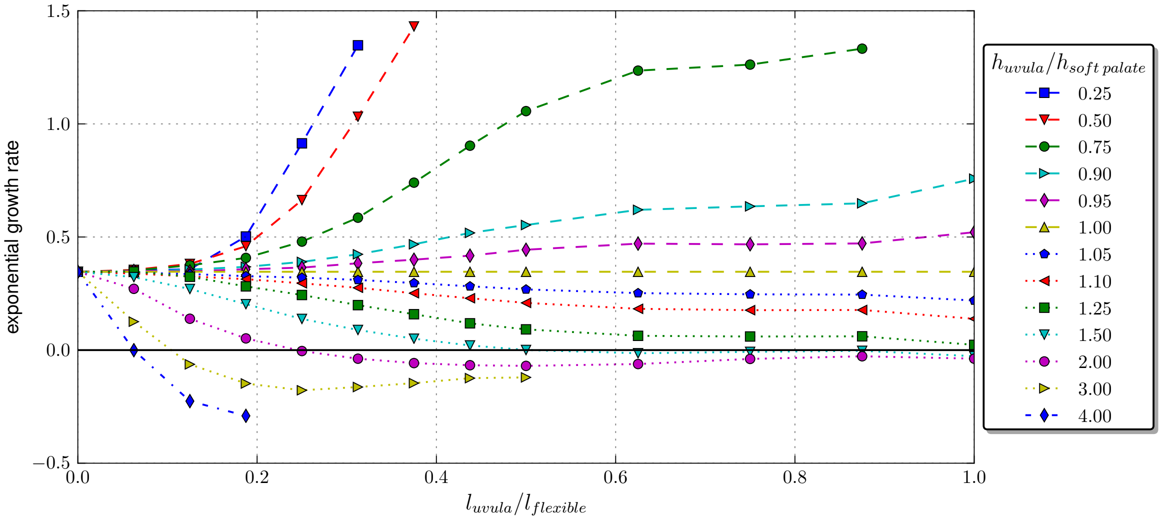

Figure 4: Exponential growth rate of the oscillations of the cantilevered flexible plates as a function of the length ratio $l_{\text{uvula}}/l_{\text{flexible}}$ for several thickness ratios $h_{\text{uvula}}/h_{\text{soft palate}}$. A higher growth rate indicates a more unstable system and a negative growth rate indicates stabilisation of the FSI system.

terises the uvula, increasingly favours an unstable oscillatory motion of the soft palate, and hence the occurrence of snoring, as it gets longer. On the other hand, if a uvulopalatal system presents a strong tendency to flow-induced instability, its properties have to be significantly altered to obtain a more stable system and prevent snoring. Further investigations based on similar modelling with variations of more parameters would help elucidating the influence of higher mode shapes, and their interaction, on the FSI system stability.

Acknowledgements

The authors gratefully acknowledge financial support of the Australian Research Council through Grant DP0559408 and the WA State Center of Excellence in eMedicine (Project “Airway tomography instrumentation”).

References

[1] Balint, T. S. and Lucey, A. D., Instability of a cantilevered flexible plate in viscous channel flow, *J Fluid Struct*, **20**, 2005, 893–912.

[2] Berry, D. A., Moon, J. B. and Kuehn, D. P., A finite element model of the soft palate., *Cleft Palate Craniofac J*, **36**, 1999, 217–223.

[3] Birch, M. J. and Srodon, P. D., Biomechanical properties of the human soft palate, *Cleft Palate-cran J*, **46**, 2009, 268–274.

[4] Cheng, S., Gandevia, S. C., Green, M., Sinkus, R. and Bilston, L. E., Viscoelastic properties of the tongue and soft palate using MR elastography, *J Biomech*, **44**, 2011, 450–454.

[5] De Backer, J. W., Vos, W. G., Verhulst, S. L. and De Backer, W., Novel imaging techniques using computer methods for the evaluation of the upper airway in patients with sleep-disordered breathing: A comprehensive review, *Sleep Med Rev*, **12**, 2008, 437–447.

[6] Elliott, N. S. J., Lucey, A. D., Heil, M., Eastwood, P. R. and Hillman, D. R., Modelling and simulation of fluid-structure interactions in human snoring, in *9th International Congress on Modelling and Simulation (MODSIM 2011)*, 2011.

[7] Heil, M. and Hazel, A. L., `oomph-lib` – an object-oriented multi-physics finite-element library, in *Fluid-Structure Interaction*, editors M. Schäfer and H.-J. Bungartz, Springer, 2006, 19–49.

[8] Howell, R. M., Lucey, A. D., Carpenter, P. W. and Pitman, M. W., Interaction between a cantilevered-free flexible plate and ideal flow, *J Fluid Struct*, **25**, 2009, 544–566.

[9] Huang, Y., White, D. P. and Malhotra, A., The impact of anatomic manipulations on pharyngeal collapse. Results from a computational model of the normal human upper airway, *Chest*, **128**, 2005, 1324–1330.

[10] Reda, M., Sims, A. J., Collins, M., McKee, G. J., Marshall, H., Kelly, P. J. and Wilson, J. A., Morphological assessment of the soft palate in habitual snoring using image analysis, *The Laryngoscope*, **109**, 1999, 1655–1660.

[11] Svaza, J., Skagers, A., Cakarne, D. and Jankovska, I., Upper airway sagittal dimensions in obstructive sleep apnea (osa) patients and severity of the disease, *Stomatologija*, **13**, 2011, 123–127.

[12] Tetlow, G. A. and Lucey, A. D., Motions of a cantilevered flexible plate in viscous channel flow driven by a constant pressure drop, *Commun Numer Meth En*, **25**, 2009, 436–482.

[13] Wang, Y., Wang, J., Liu, Y., Yu, S., Sun, X., Li, S., Shen, S. and Zhao, W., Fluid-structure interaction modeling of upper airways before and after nasal surgery for obstructive sleep apnea, *Int J Numer Method Biomed Eng*, **28**, 2012, 528–546.

[14] Zhu, J. H., Lee, H. P., Lim, K. M., Lee, S. J., Teo, L. S. L. and Wang, D. Y., Passive movement of human soft palate during respiration: A simulation of 3D fluid/structure interaction, *J Biomech*, **45**, 2012, 1992–2000.